DESGIN AND FABRICATION OF A THREE DIMENSIONAL VALVELESS MICROPUMP WITH SHAPE DEPOSITION MANUFACTURING PROCESS (SDM)

Sanjay Kumar Jha*

Balvinder*

Rupak Kumar Deb**

Dr. Vinay Chandra Jha**

Dr. Iqbal Ahmed Khan***

ABSTRACT

The present work is focused on manufacture of three-dimensional valveless micropump with inexpensive approach. The design of the micropump is such that it consists of three horizontal inlet channels and one outlet (vertical) channel. The 3D geometry of the channels with minimum width of 80 μm gives great challenges in fabrication and is difficult to be achieved by traditional fabrication techniques. For manufacture the chamber and channels of the micropump the Shape Deposition Manufacturing (SDM) process, a layered manufacturing technique is involved into the repeated material deposition and removal. CAD/CAM software is used to slice the 3D model and plan the manufacturing sequences. The piezoelectric buzzer was attached to the fabricated valveless micropump chamber to test the performance. Three different channel width designs were manufactured successfully and tested at various piezo-triggered frequencies.

This research provides a solution to manufacture the three-dimensional micropump geometry inexpensively. SDM process was proved to be a suitable approach to generate pre-assembled valveless micropump structure with micro channels, and is applicable to other similar applications also.

Keyword: *Micropump, Design, Fabrication, 3D, Manufacturing.*

*Gold Field Institute of Technology and Management, Faridabad, India.

**Lingaya's University, Faridabad, Haryana, India.

***Greater Noida Institute of Technology, Greater Noida, U.P.

INTRODUCTION

Micropumps have been developed for more than two decades. Their characteristic of handling small and precise volumes of liquid and/or gas makes them able to serve chemical, medical, and biomedical applications with great scientific and commercial potential. Fuel delivery in a fuel cell system [1], drug delivery [2], and integration with miniaturized chemical analyzers as a "Micro total analysis system (_TAS)"[3] are some of the examples.

The design of micro pumps can be divided into valve based and valve less. In valve-based pumps, mechanical check valves in terms of membranes or flaps are used. Wear, fatigue, and valve blocking are issues concerned in this type and limit its applications. Valve less micro pumps, first introduced by Stemme and Stemme [4], use diffuser/nozzle elements to perform as a check valve. The construction of valve less micro pumps is relatively simple compared to check valves and can avoid the problems mentioned above. Most common actuation methods in micro pumps include electromagnetic [5], electrostatic [6], shape memory alloy [7], thermo-pneumatic [8], and piezoelectric [4,9–10]. Piezoelectric actuation can provide relatively a high actuation force and a fast mechanical response, therefore, is widely used in micro pump development.

Micro-electro-mechanical system (MEMS) technologies are the major manufacturing approach to build micro pumps in recent researches. Silicon micromachining and polymer-based micromachining techniques are the main categories. Silicon moving parts can avoid wear and fatigue problems in the long-run tests, but the material choice is limited and fabrication cost is relatively high. In polymer micro-fabrication, such as thick-resist lithography, soft lithography, micro stereo-lithography, and micro injection molding, the advantage is the possibility of using different polymeric materials to meet biocompatibility and chemical resistance for its potential applications. However, the limited material lifetime can be an issue and the goal of true low-cost micro pump is still not achieved yet. Besides, most of the MEMS techniques can only build 2.5-dimensional geometry rather than a true three-dimensional one. The micro-channel geometry was hence limited in the most designs. Therefore, there is a need to develop some manufacturing alternatives which are capable of building true 3D geometry at lower cost.

In this research, we focused on manufacture of threedimensional valveless micropumps in inexpensive approach. A special micropump design with vertical and horizontal diffusers/nozzles is proposed initially as a micro-submarine's propulsion system, but is not limited to this specific application. A manufacturing alternative, shape deposition

manufacturing (SDM) process, which can build true 3D geometry, was applied to fabricate pre-assembled chamber with inlet and outlet channels. Moreover, three valveless micropump designs with different channel width were fabricated and tested.

ACTUATING PRINCIPLE

Up to now almost the whole range of microactuation techniques available have been used for the design of micropumps. Common principles include piezoelectric [16–18,19,40,42], thermopneumatic [20–21], electrostatic [20–23] and electromagnetic actuation [24,25], whereas some others, like shape memory [26] or magnetostrictive effects are rarely found.

Piezoelectric actuation was the first actuation principle used in micropumps. It is a very attractive concept, as it provides a comparatively high stroke volume, a high actuation force and a fast mechanical response. Moreover, commercial PZT material is readily available for a hybrid integration. The comparatively high actuation voltage and the mounting procedure of the PZT disk can be regarded as disadvantages. A systematic optimization of the mounting process can significantly improve reliability and yield of this type of actuator [27,28]. Nevertheless, hybrid integration requires a very well-defined glueing which is critical for the actuator performance and not easily done. Therefore, screen printing [24,25] and thin-film deposition of PZT material have been studied as an alternative quasi-monolithic integration technique. Although the feasibility of these techniques could be demonstrated, the resulting strokes (e.g. 1_m at 100V in [24]) are small in comparison to glued PZT bulk material (e.g. 15 _m at 100V in [30]). Optimization of the geometrical design was done at several places to achieve higher strokes at lower voltages [11,26]. Typical actuation voltages of such optimized design are in the range of 100V (e.g. 130VPP for the micropump in [23]), which is a significant improvement in comparison to other micropumps that sometimes use commercial piezo buzzers without any optimisation (e.g. 400VPP for the micropump in [23]). This lower actuation voltage is also helpful for the design of highly miniaturized electronic drivers which allow low-power operation from a battery [22].

As a second concept thermopneumatic actuation was first demonstrated by Van de Pol et al. [7] with a micropump similar to Van Lintels device. Instead of a PZT disk an air-filled chamber with an internal heater resistor was integrated on top of the pump diaphragm. The heater is realized either as a free-hanging structure [7–9] to achieve a better thermal efficiency or simply attached to the pump diaphragm [10]. This type of actuator represents a low-voltage alternative to the piezoelectric drive and does not require big efforts concerning the electronic driver [7]. Moreover, thermopneumatic actuators can be made very compact

[10], but are nevertheless capable to generate strokes up to several 100 _m to achieve high pump rates [8]. Integration into standard silicon processing is easily achieved [9]. A crucial drawback of this actuation principle is a relatively long thermal time constant, especially during the cooling process. This limits the upper actuation frequency to approximately 50 Hz. The typical electrical power consumption is in the range of several watts which usually excludes portable operation from a battery. Also, at these power levels a heating of the transported medium can not be excluded. Fig. 5 shows the first practically successful micropump with electrostatic actuation from Zengerle et al. [19], who also realized the first vertically-stacked modular micropump design in silicon. The actuator is made from two silicon chips that embody the flexible pump diaphragm and a rigid counter electrode in a capacitor-like configuration. Applying high voltage to the capacitor electrodes causes electrostatic attraction of the pump diaphragm which in extreme gets fully attached to the counter electrode. After discharge of the capacitor the pump diaphragm relaxates to its rest position.

With this rapid actuation principle bidirectional pumping was observable at high operation frequencies caused by a time delay between the diaphragm movement and the somewhat slower valve switching [19].

Electrostatic actuation offers operation frequencies up to several kHz, an extremely low power consumption and full MEMS compatibility [18–20]. A major disadvantage results from the inherently small actuator stroke, which is usually limited to practical values around 5 _m with corresponding actuation voltages around 200V. Also degradation of the actuator performance is found sometimes in long-term high voltage operation. This is due to the build-up of surface charges at the insulator inside the capacitor, which reduce the internal electrical field strength and, therefore, the stroke. Bipolar operation is a practical solution to overcome this problem at the prize of a more complex electronic driver.

Electromagnetic actuation is used sometimes [16,17]. Although not well compatible with MEMS integration, this actuation concept can easily be adapted in a modular way and offers the benefit of a separate optimisation of micropump and actuation unit. The two references cited here use a permanent magnet attached to the pump diaphragm that is moved by an external coil. The overall electrical and mechanical properties are comparable to thermopneumatic actuators with the advantage of a slightly faster mechanical response.

VALVE DESIGN

In the MEMS devices demonstrated above mechanical check valves were used, either with membranes or with flaps. The effort to design and fabricate such valves should not be underestimated. A number of critical properties like backward flow, pressure drop and switching speed have to be kept under tight control to achieve a working micropump. Moreover, wear and fatigue can be a critical issue, especially in polymer-fabricated devices. There is also the risk of valve blocking by even small particles, which instantly degrade the pumping performance. This limits the application range of most valve-based micropumps to filtered media.

The so-called "valveless" micropump concept can avoid these problems. The device was introduced by Stemme and Stemme [27]. It uses diffuser/nozzle elements with flow-rectifying properties to mimic the function of a check valve (Fig. 6). According to [27] a maximum achievable forward–backward flow ratio of 2.23 can be calculated for this type of "valve" which is sufficient for a pumping effect. The prototype shown in Fig. 6 was fabricated from a cylindrical brass body with an outer diameter of 29mm and tested with two different diffuser/nozzle geometries. The theoretically calculated forward-to-backward flow ratios of 1.48 and 1.67 agreed well with the experimental data. A remarkably high zero-pressure flow of 11 ml/min and a maximum outlet pressure of approximately 100 mbar were found for water, depending on the diffuser/nozzle geometry in use. This micropump was also able to pump gases.

Based on this prototype various planar silicon micropumps were realized in the following. To reduce inlet and outlet pressure pulses and to increase the pump flow performance, a set-up of two valveless micropumps was realized by Olsson et al. [28,29]. Another planar design was developed by Foster et al. [30] on the basis of a more complicated flow-rectifying valve structure proposed by Tesla [31]. Vertically-stacked devices are originating from the work of Gerlach et al. [32] and, later on, Koch et al. [25]. They use the conical sidewalls of anisotropically etched silicon cavities to build a diffuser/nozzle element with no additional technological effort. A theoretical treatment of the pump principle in conjunction with the corresponding diffuser/nozzle elements is available in a number of publications [30,32–34].

The advantage of valveless micropumps is a relatively simple construction in comparison to pump concepts with check valves or active valves. The pumping of particle loaded media or sensitive material is easier to achieve due to the open flow structures. These benefits are, however, accompanied by the lack of self-blocking. Any overpressure at the outlet will cause

reverse flow that becomes predominant when the pump is switched off. A “valve-less micropump” with improved blocking capability was found by Stehr et al.[35,36], who discovered and evaluated the pumping effect of a bossed silicon diaphragm valve that was periodically actuated by a piezoelectric bimorph. Here the dynamic modulation of the gap width between boss and valve seat does result in a flow-rectifying behavior. The device was able to transport liquids and gases. The pumping direction could be reversed by a variation of the actuation frequency. Reverse flow in the off state could be prevented to a certain extent by simply closing the valve. During operation however, reverse flow was present as in the other valveless designs.

MATERIALS AND FABRICATIONS TECHNIQUE

After the early designs which were realized by conventional machining [1,2], micropump fabrication has soon become an almost exclusive domain for silicon micromachining. Micromachined silicon and glass have been used advantageous due to the high geometric precision available with this technology. Aside from that long-term tests have shown that wear and fatigue of mechanically moving parts, e.g. valve flaps, does not occur in silicon micropumps [12,22]. From this reason, true high performance applications, e.g. in drug delivery, can still be regarded as a clear domain of silicon micromachining as demonstrated by recent industrial efforts in this direction [40,41]. However, the disadvantages of a rather high fabrication cost and a limited material choice have stimulated the search for alternatives. In the meantime polymer microfabrication, namely microinjection moulding [10,13,42], polymer hot embossing [43] and stereolithography [15,16] have been demonstrated as alternative technologies for micropump fabrication. However, the goal of a true “low-cost” micropump, although often promised, is not satisfied with several of these technologies which are still highly complex and therefore comparatively expensive microfabrication processes. Moreover, other material-related aspects, like limited lifetime can be a critical issue.

In this situation an interesting pragmatic concept was presented by Piet Bergveld’s group with the work of Böhm et al. [14,17] who has also done successful research on the later described electrochemical pumping principle. Instead of polymer microfabrication they have used conventional polymer molding as a true low cost method to realize micro diaphragm pumps with piezoelectric and electromagnetic actuation. Other research is using well-established printed circuit board technology for the realization of micropumps and microfluidic devices [8]. These concepts may not provide the performance of thoroughly

designed silicon devices, but will definitely deliver an acceptable result at very moderate fabrication costs. They seem to be an interesting choice for all moderate-performance and low-cost applications, provided that other requirements, like reproducibility and operational stability, can be satisfied.

DESIGN OF VALVELESS MICROPUMP

The micropump developed in this research is a piezoelectric actuated valveless pump. This pump consists of a chamber, three horizontal inlet channels, and one vertical outlet channel. This was originally designed for propelling a micro-submarine with the configuration of inlets from the side perpendicular to one outlet in the back as shown in fig 4.

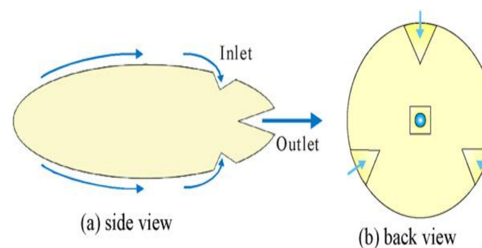

Fig 4. Schematic drawings of a valveless micropump placed at the end of a micro-submarine with three inlets and one outlet.

Diffuser Design

In the traditional valveless micropump, the working theory can be illustrated in Fig. 6. The dimension difference at the both ends of the diffuser causes the pressure difference and drives the fluid. In the supply mode, the actuator increases the chamber volume, resulting in a lower pressure inside the chamber. In this situation, the inlet flow is greater than the outlet flow; therefore, the fluid is supplied into the chamber. Reversely, in the pump mode, the decrease in the chamber volume increases the chamber pressure and, as a result, the outlet flow is greater than the inlet flow.

The diffuser/nozzle design determines the performance of the micropump. Diffusers can be categorized as conical and flat walled with circular and rectangular cross-section, respectively. The length of the flat walled diffuser will be 10–80% shorter than that of the conical one under the same flow performance. Therefore, flat-walled diffuser design was chosen in this research. The major dimensions of a diffuser with the same channel height b include throat width $W1$, exit width $W2$, length L, and total included diffuser angle 2θ.

According to the stability map of a diffuser, the diffuser operates in four different regions depending on the diffuser geometry. In the bi-stable steady stall (between b–b and c–c lines) and jet flow (above c–c line) regions, the flow performance is poor to extremely poor. Under the line a–a, the no stall region, the flow is steady viscous without separation at the diffuser

walls and a moderate performance is achieved. In the transitory steady stall region between a–a and b–b lines, the flow is unsteady. Minimum pressure loss and maximum pressure-recovery coefficient *C*p occur in this region, and hence the diffuser geometry will be designed accordingly. The typical performance map for a flat walled diffuser is shown in Fig. 5. The AR is defined as the area ratio between exit and throat. From the map, the maximum *C*p occurs when $L/W1$ is between 16 and 18, 2θ is around 10◦, and AR falls between 3.5 and 4. Therefore, the diffuser geometry was designed to be $L/W1 = 16$, AR= 3.5, and 2θ =10◦.

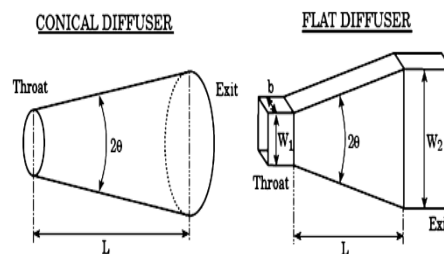

Fig 5. Conical and Flat Walled Diffuser

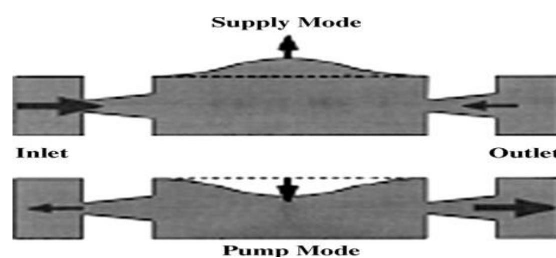

Fig 6. Working Principle of Valveless Micropump

Piezoelectric actuator

A commercial available piezoelectric buzzer was used as the actuator. The buzzer, illustrated in Fig. 7, consists of a brass layer for resonance and a piezoelectric ceramic layer with a sliver coating for external-drive connection. In order to keep the overall size of the micropump small, the smallest diameter available was selected.

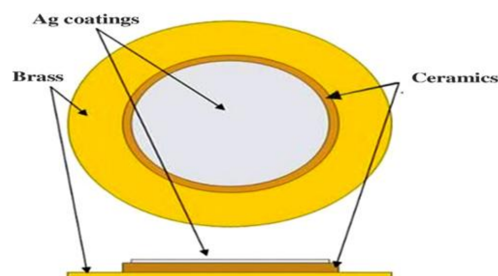

Fig 7. Piezo-electric Buzzer

The Diameter of the Brass Layer is 9 mm and that of the Ceramic Layer is 6 mm. The thickness is 0.2 mm.

Micropump design

The exploded view of the final micropump design and its component list are shown in Fig. 8. The chamber is 8mm in diameter due to the dimension of the selected piezoelectric buzzer, and 110μm in height. Three inlet channels are located at the side of the chamber and a outlet channel is placed at the bottom with the channel height b three times of that for inlet channels to balance the flow amount. The general view and the cross-section view of the micropump's chamber and channels are shown in Fig. 9.

The length L is calculated based on $L/W1 = 16$. The exit channel width ($W2$), which is not listed in the table, can be determined by $W1$, 2θ, and L.

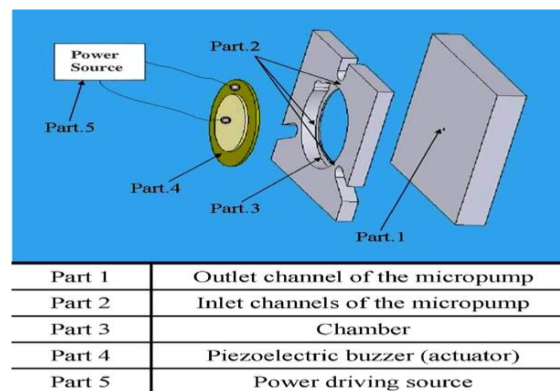

Part 1	Outlet channel of the micropump
Part 2	Inlet channels of the micropump
Part 3	Chamber
Part 4	Piezoelectric buzzer (actuator)
Part 5	Power driving source

Fig 8. Exploded view of micropump and component list.

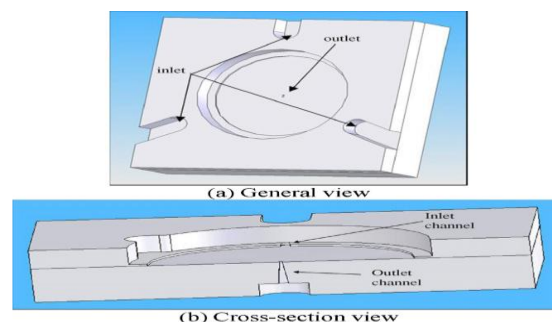

Fig 9. General view and cross-section view of micropump

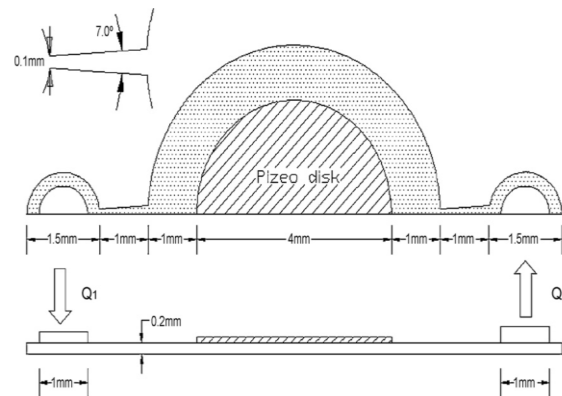

Fig 10. Configuration of Valveless Micropump

RESULTS

The settings of the geometry of the micropump are given in Fig. 10. It is assumed that the membrane reciprocates in a harmonic motion with a frequency of 2200 Hz. The maximum amplitude of the vibration is 1.0μm. The large ratio of the chamber height to the vibration amplitude justifies the use of moving velocity instead of moving surface as the boundary condition. Zero pressure is specified at the inlet and various back pressures Pb, ranging from 0 to 5900 Pa, are set at the outlet. Calculations were undertaken for a number of periods. The net flow rates averaged over each period for different levels of grid are given in Fig 11. for the case with $Pb = 0$. It can be observed that it takes at least three periods for the flow to become fully periodic.

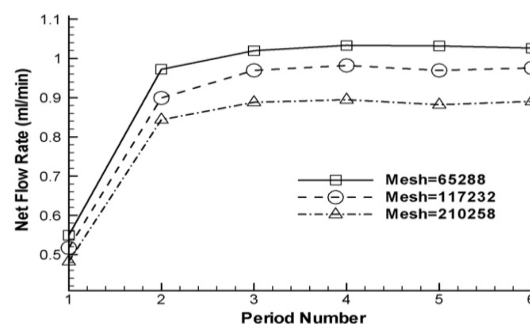

Fig 11. The net flow rates in each period for different levels of grid for the case Pb =0.

The pumping effect caused by the valveless micropump becomes clear by viewing the variation of the flow rates $-Q1$ (negative value of $Q1$) and $Q2$, as shown in Fig. 12. For the case $Pb = 0$ the flowrate at the outlet $Q2$ is higher than the flowrate at the inlet $-Q1$ in the first half of a period (the pumping stage) due to the diffuser function of the element connecting the outlet chamber and the nozzle function of the element connecting the inlet chamber. In the

second half of the period, the absolute value of $Q2$ becomes lower than that of $Q1$ because the flow direction is reversed (the supply stage). The flow rate $Q2$ can be approximately expressed by a sinusoidal function a + b sinωt and the flowrate$-Q1$ by$-a$ + b sinωt. The constant a represents the net flow rate. For the case Pb =5310Pa the variations of the flow rates $-Q1$ and $Q2$ are very close to each other and the net flow rate, or the constant a, approaches zero.

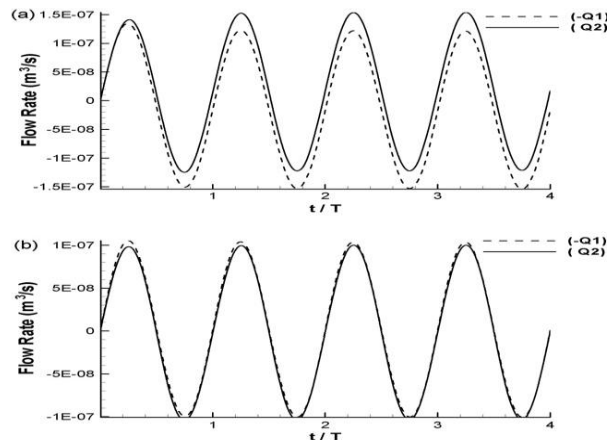

Fig. 12. Variation of the flow rates at the inlet (Q1) and outlet (Q2) for (a) Pb = 0 and (b) Pb =5310Pa.

To illustrate the flow field, the plots of streamlines and pressure contours in the two nozzle/diffuser regions at t = T/4 and 3T/4 are shown in Figs. 13 and 14, respectively. At t = T/4 in the pumping stage, the flow is directed from the main chamber toward the inlet and the outlet chambers. The discharge element on the left functions as a nozzle and that on the right as a diffuser. The pressure decreases gradually is the nozzle whereas the pressure drops sharply at the entrance of the diffuser and then recovers gradually. It can be seen that there exists a recirculation zone near the entrance corner in the nozzle and another recirculation zone before the fluid enters the nozzle. The former is caused by the sharp entrance while the latter is due to the fact that as seen in Fig. 14 for t=3T/4, the recirculation formed by the flow emerging from the nozzle/diffuse element in the supply stage persists and moves down toward the central region during the pump stage. The recirculating flow leads to a low pressure region at the entrance of the nozzle and, thus, causes additional losses. The flowtype is reversed in the supply stage at t=3T/4. It can be detected that both the velocity and pressure fields in Fig. 17 are very similar to those in Fig. 16 except that the roles of the two nozzle/diffuser elements are interchanged.

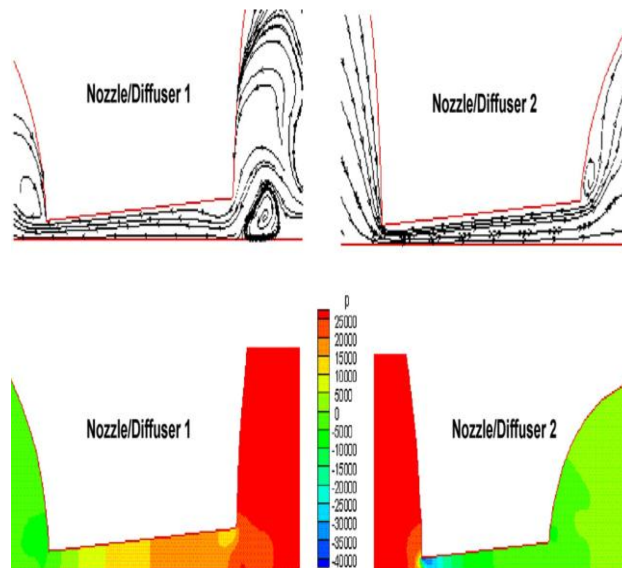

Fig. 13. The plots of streamlines and pressure contours in the two nozzle/diffuser regions at t = T/4.

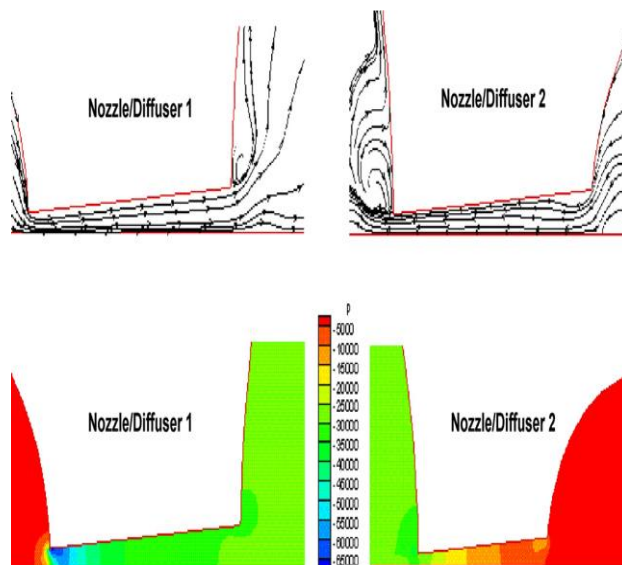

Fig. 14. The plots of streamlines and pressure contours in the two nozzle/diffuser regions at t=3T/4.

The multidimensional solution procedure is validated by comparing the predicted net flow rates with the measurements of Olsson et al. [7], as shown in Fig. 10. The calculations were performed using the parabolic, trapezoidal, and blending profiles, as given by Eq. (7). As expected, the net flow rates decrease when the back pressure increases. In general, the flowrates are overpredicted by using the trapezoidal profile, especially for sufficiently large Pb, and underpredicted when the parabolic profile is employed. The higher flow rate obtained

by using the trapezoidal profile is due to its larger volume displacement. The strategy in the blending profile is to use the trapezoidal profile at *P*b = 0, the parabolic profile at *P*b = 5900 Pa, and a linear combination of the two in between. As seen from the figure, the resulting flow rates become much closer to the experiment data.

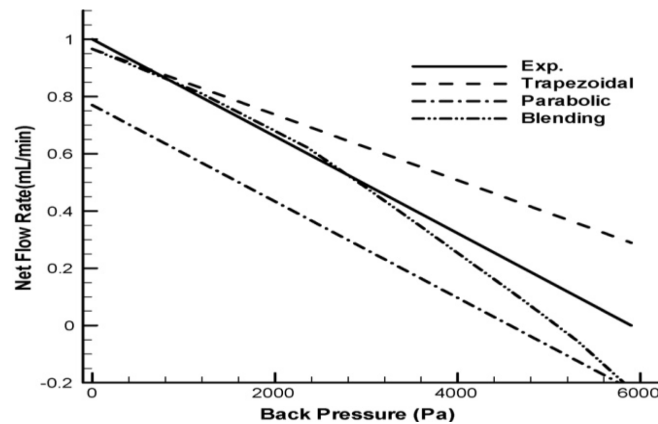

Fig. 15. Comparison of predicted net flow rates using different membrane profiles with measurements at various back pressures.

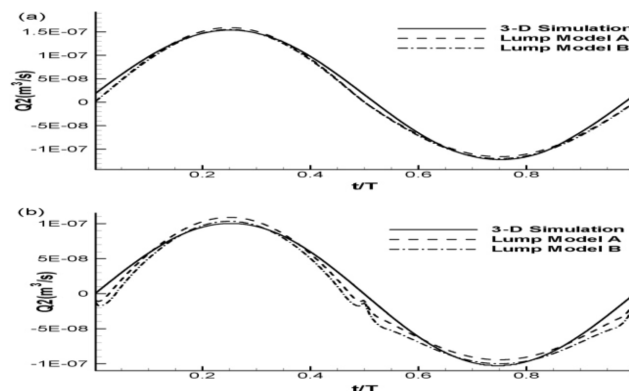

Fig. 16. Variation of the flow rates at the outlet in one period predicted by the 3D simulation and the two lump models for (a) Pb = 0 and (b) Pb =5310Pa.

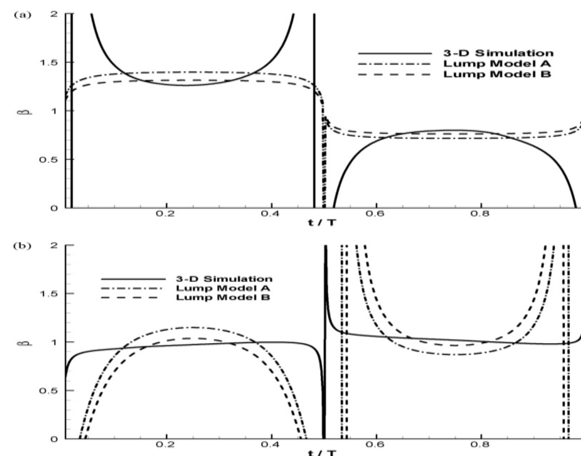

Fig. 17. Comparison of the flow rate ratios ˇ in one period obtained by the 3D simulation and the two lump models for (a) Pb = 0 and (b) Pb =5310Pa.[40]

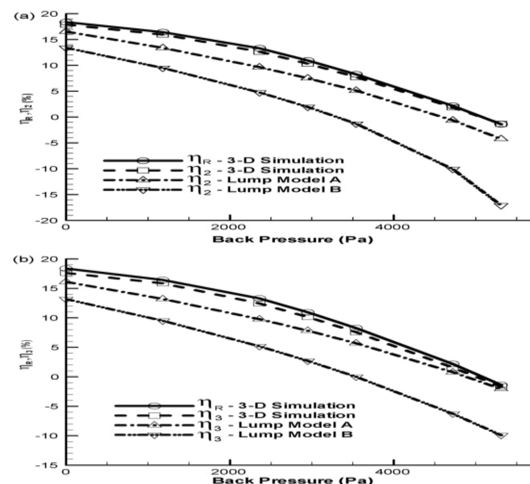

Fig. 18. Comparison of the predicted efficiencies η_2 and η_3 by the 3D simulation and the two lump models

MANUFACTURING OF THE MICROPUMP

Challenges in manufacturing

In the previous researches, the micro pumps were usually designed to place the inlet and outlet diffuser/nozzle channels in the same plane. That is, the geometry is 2.5D without critical shape change in the third axis. Micro fabrication techniques are capable of fabricating these features and are often utilized in these applications even though the cost may be relatively high in the prototyping stage. However, for the specific design in this research, inlet and outlet channels are placed in 3D space. Most of the micromachining methods are 2.5D and will introduce steps between layers, which means they are incapable of producing

smooth 3D surfaces for diffuser channels. Besides the 3D geometry, the minimum channel width of 80 µm and the high aspect ratio of the vertical channel also give great challenges in manufacturing.

Material and process selection

In material selection, polymers are the top choice due to its ease of shaping and machining. Three possible processes can be used to shape complex parts—parts can be machined from available bulk material, can be injection molded, or can be cast. In our micro pump design, the machining approach will need additional assemblies of the chamber and channels. Alignment is an issue and special fixture is required. The high cost of die makes injection molding not economically favored in low volume production. Casting is a feasible approach if suitable molding techniques are applied. Room-temperature-cured polymers are preferred because they reduce the need of furnace and special temperature control systems. Molds can be permanent or fugitive. Fugitive molds are more flexible and mold release can be done by chemical or thermal means. As a result, shape deposition manufacturing process [16], developed by Carnegie Mellon University and Stanford University, and provides a solution for room-temperature polymer casting.

SDM is a layer manufacturing technique with a sequence of additive and subtractive processing steps for fabricating complex 3D parts. In each layer, part material or support material are deposited and machined to net shapes. After the part is completely built, the support material is removed chemically or thermally, depending on the material characteristics. Various materials, such as metals and polymers, can be fabricated by SDM.

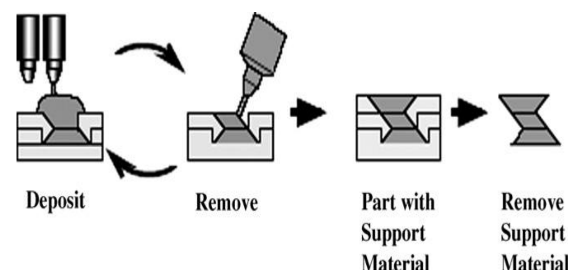

Fig 19. Shape Deposition Method

Since the original polymer part materials used by Stanford University's Rapid Prototyping Laboratory [17] are not commercially available anymore, we searched for new part material that is room-temperature-cured with similar properties to Adtech EE-501/530 epoxy. As a result, Ciba FC 52Isocynate/52Polyol was chosen. It takes 60–90 min to cure, and the density is 1.6–1.7 g/cm3. Other properties are listed in Table 3. The support material used in this research is the same as that used at Stanford, a combination of 25% File-a-wax and 75%

Proto-wax. The support material is removed by BIOACT 280 at 70 ◦C with ultrasonic vibration.

Manufacturing approaches

The manufacturing of the chamber with inlet and outlet channels were divided into three sections—bottom, middle, and top. The bottom section contains a vertical outlet channel with high- aspect ratio (Fig. 10), which is the most difficult to manufacture among three sections. The middle section includes inlet channels, while the top section includes the main chamber body and the fixture feature for integration with the actuator. Three sections are built sequentially. The support material, wax, was removed at the end to obtain a chamber with inlet and outlet channels without assembly.

In the bottom section, the vertical outlet channel is filled by support material, wax. Since the channel dimension is very small, it is hard to find a suitable cutting tool to machine the cavity out of the part material and then pour in support material. Therefore, the SDM process planning implemented this section into two stages. In the first stage, a wax substrate rather than a polymer substrate was used. The wax substrate was machined up to channel's partial surfaces, and the part material was cast to fill up the machined area. The second stage machined the other portion up to channel's remaining surfaces, and cast in the cavity with the part material. In this approach, the channel area was the only wax region left as we wanted. Since the region to be machined is larger than the available tool size, general end-mills can be used directly and no special small cutting tool is required. The next issue is to determine the portion for the first stage. Due to the small wax region left during and after machining in the second stage, it is very likely to break off during machining.

Therefore, more bonding surfaces to the first-stage part material can provide stronger bonding and are preferred. As a result, two consecutive surfaces were selected as the machining boundary surfaces for the first stage, and the other two surfaces were for the second stage. The arrow direction shows the portion to be machined away in each stage.

In the middle section, support material was deposited on the bottom section and machined to define the geometry of inlet channels. Since these channels are placed horizontally, there are no high-aspect ratio and bonding issues, and one round of support material deposition and machining is sufficient. The top section was done by casting the part material and machining to the required shape.

CONCLUSIONS

In this research, a new valve less micro pump design was proposed with three inlets perpendicular to one outlet. With this 3D feature, common micro-fabrication techniques which can only generate 2.5D geometry are not applicable. As a result, a layered manufacturing technique, SDM process, was utilized to fabricate 3D micro-channels successfully and was proven to be a suitable approach to generate pre-assembled valve less micro pump structure. After attached to a piezoelectric buzzer, three types of working micro pumps designed with different channel widths were tested at various frequencies.

REFERENCES

1. T. Zhang, Q. Wang, Valveless piezoelectric micropump for fuel delivery in direct methanol fuel cell (DMFC) devices, J. Power Sources 140 (2005) 72–80.
2. D. Maillefer, S. Gamper, B. Frehner, P. Balmer, H. van Lintel, P. Renaud, A high-performance silicon micropump for disposable drug delivery systems, in: The 14th IEEE International Conference on MEMS, 2001.
3. A. Manz, N. Graber, H.M. Widmer, Miniaturized total chemical analysis systems: a novel concept for chemical sensing, Sens. Actuators B 1 (1990) 244–248.
4. E. Stemme, G. Stemme, A valveless diffuser/nozzle-based fluid pump, Sens. Actuators A 39 (1993) 159–167.
5. J. Jang, S. Lee, Theoretical and experimental study of MHD (magnetohydrodynamic) micropump, Sens. Actuators A 80 (2000) 84–89.
6. R. Zengerle, J. Ulrich, A bi-directional silicon micropump, Sens. Actuators A 50 (1995) 81–86.
7. D. Xu, L. Wang, Characteristics and fabrication of NiTi/Si diaphragm micropump, Sens. Actuators A 93 (2001) 87–92.
8. A. Wego, L. Pagel, A self-filling micropump based on PCB technology, Sens. Actuators A 88 (2001) 220–226.
9. M.C. Acero, J.A. Plaza, J. Esteve, M. Carmona, S. Marco, J. Samitier, Design of a modular micropump based on anodic bonding, J. Micromech. Microeng. 7 (1997) 179–182.
10. B. Büstgens, W. Bacher, W. Bier, R. Ehnes, D. Maas, R. Ruprecht, W.K. Schomburg, L. Keydel, Micromembrane pump manufactured by molding, in: Proceedings of the Actuator '94, Bremen, Germany, 15–17 June 1994, pp. 86–90.

11. R. Linnemann, P. Woias, C.-D. Senfft, J.A. Ditterich, A self-priming and bubble-tolerant silicon micropump for liquids and gases, in: Proceedings of the MEMS '98, Heidelberg, Germany, 25–29 January 1998, pp. 532–537.
12. P. Woias, R. Linnemann, M. Richter, A. Leistner, B. Hillerich, in: D.J. Harrison, A. van den Berg (Eds.), Micro Total Analysis Systems '98, Kluwer Academic Publishers, Dordrecht, 1998, pp. 383–386.
13. J. Döpper, M. Clemens, W. Ehrfeld, K.-P. Kämper, H. Lehr, Development of low-cost injection moulded micropumps, in: Proceedings of the Actuator '96, Bremen, Germany, 26–28 June 1996, pp. 37–40.
14. S. Böhm, M. Dierselhuis, W. Olthuis, P. Bergveld, in: D.J. Harrison, A. van den Berg (Eds.), Micro Total Analysis Systems '98, Kluwer Academic Publishers, Dordrecht, 1998, pp. 391–394.
15. M.C. Carrozza, N. Croce, B. Magnani, P. Dario, A piezoelectricallydriven stereolithography-fabricated micropump, J. Micromech. Microeng. 5 (1995) 177–179.
16. P. Dario, N. Croce, M.C. Carrozza, G. Varallo, A fluid handling system for a chemical microanalyzer, Technical Digest of the MME '95, Sixth Workshop on Micromachining, Micromechanics and Microsystems, Copenhagen, Denmark, 3–5 September 1995, pp. 140–143.
17. S. Böhm, W. Olthuis, P. Bergveld, A plastic micropump constructed with conventional techniques and materials, Sens. Actuators 77 (1999) 223–228.
18. J. Judy, T. Tamagawa, D.L. Polla, Surface-machined micromechanical membrane pump, in: Proceedings of the MEMS '91, Nara, Japan, 30 January–2 February 1991, pp. 182–186.
19. R. Zengerle, S. Kluge, M. Richter, A. Richte, A bidirectional silicon micropump, in: Proceedings of the MEMS '95, Amsterdam, The Netherlands, 29 January–2 February 1995, pp. 19–24.
20. T. Bourouina, A. Bosseboeuf, J.-P. Grandchamp, Design and simulation of an electrostatic micropump for drug-delivery applications, J. Micromech. Microeng. 7 (1997) 186–188.
21. E. Makino, T. Mitsuya, T. Shibata, Fabrication of TiNi shape memory micropump, Sens. Actuators A 88 (2001) 256–262.
22. S. Kluge, G. Neumayer, U. Schaber, M. Wackerle, M. Maichl, P. Post, M. Weinmann, R. Wanner, Pneumatic silicon microvalves with piezoelectric actuation, in: Proceedings

of the Transducers '01/Eurosensors XV, Munich, Germany, 10–14 June 2001, pp. 924–927.

23. M. Richter, J. Kruckow, J. Weidhaas, M. Wackerle, A. Drost, U. Schaber, M. Schwan, K. Kühl, Batch fabrication of silicon micropumps, in: Proceedings of the Transducers '01/Eurosensors XV, Munich, Germany, 10–14 June 2001, pp. 936–939.
24. M. Koch, N. Harris, A.G.R. Evans, N.M. White, A. Brunnschweiler, A novel micromachined pump based on thick-film piezoelectric actuation, in: Proceedings of the Transducers '97, vol. 1, Chicago, USA, 16–19 June 1997, pp. 353–356.
25. M. Koch, A.G.R. Evans, A. Brunnschweiler, The dynamic micropump driven with a screen printed PZT actuator, J. Micromech. Microeng. 8 (1998) 119–122.
26. C.J. Morris, F.K. Forster, Optimization of a circular piezoelectric bimorph for a micropump driver, J. Micromech. Microeng. 10 (2000) 459–465.
27. E. Stemme, G. Stemme, A valveless diffuser/nozzle-based fluid pump, Sens. Actuators A 39 (1993) 159–167.
28. N.-T. Nguyen, X. Huang, T.K. Chuan, MEMS-micropumps: a review, ASME J. Fluids Eng. 124 (2002) 384–392.
29. D.J. Laser, J.G. Santiago, A review of micropump, J. Micromech. Microeng. 14 (2004) R35–R64.
30. P. Woias, Micropumps—past, progress and future prospects, Sens. Actuator B 105 (2005) 28–38.
31. E. Stemme, G. Stemme, A valveless diffuser/nozzle-based fluid pump, Sens. Actuator A 39 (1993) 159–167.
32. T. Gerlach, H. Wurmus, Working principle and performance of the dynamic micropump, Sens. Actuator A 50 (1995) 135–140.
33. A. Olsson, G. Stemme,E. Stemme,Avalve-less planar fluidpump with twopump chambers, Sens. Actuator A 46–47 (1995) 549–556.
34. A. Olsson, O. Larsson, J. Holm, L. Lundbladh, O. Ohman, G. Stemme, Valve-less diffuser micropumps fabricated using thermoplastic replication, Sens. Actuator A 64 (1998) 63–68.
35. A. Ullmann, The piezoelectric valve-less pump-performance enhancement analysis, Sens. Actuator A 69 (1998) 97–105.
36. A. Olsson, G. Stemme, E. Stemme, A numerical design study of the valveless diffuser pump using a lumped-mass model, J. Micromech. Microeng. 9 (1999) 34–44.

37. L.S. Pan, T.Y. Ng, G.R. Liu, K.Y. Lam, T.Y. Jiang, Analytical solutions for the dynamic analysis of a valveless micropump—a fluid–membrane coupling study, Sens. Actuator A 93 (2001) 173–181.
38. L.S. Pan, T.Y. Ng, X.H. Wu, H.P. Lee, Analysis of valveless micropumps with inertial effects, J. Micromech. Microeng. 13 (2003) 390–399.
39. N.-T. Nguyen, X. Huang, Numerical simulation of pulse-width-modulated micropumps with diffuser/nozzle elements, in: Proceedings of the International Conference on Modeling Simulation of Microsystems MSM2000, Santiego, CA, 2000, pp. 636–639.
40. K.-S. Yang, I.-Y. Chen, C.-C.Wang, Performance of nozzle/diffuser micro-pumps subject to parallel and series combinations, Chem. Eng. Technol. 29 (6) (2006) 703–710.